

# Elevated Temperature Deformation Behavior of TA7 Titanium Alloy

Yang Xiaokang, Wang Kuishe, Shi Jiamin, Wang Meng, Cai Jun, Wang Qingjuan,  
Liu Yingying

*Shaanxi Engineering Research Center of Metallurgical, Xi'an University of Architecture and Technology, Xi'an 710055, China*

**Abstract:** Isothermal compression tests in the temperature range of 1123–1273 K and the strain rate range of 0.001–1 s<sup>-1</sup> were conducted to analyze the elevated temperature deformation behavior of TA7 titanium alloy for the purpose of acquiring optimum processing parameters. Besides, a modified parallel constitutive model was put forward to illustrate the high temperature flow stress as a function of the strain rate, deformation temperature and true strain. Thereafter, the processing map which was on the basis of dynamic materials model was established. The investigation was made from the microstructure of compressed TA7 titanium alloy specimens to validate processing map. According to the results, the deformation temperature of 1223 K and strain rate of 0.001 s<sup>-1</sup> are the best processing parameters for the TA7 alloy. In addition, the instability regions are in a relatively lower temperature-higher strain rate region.

**Key words:** TA7 titanium alloy; elevated temperature deformation behavior; constitutive equation; processing map

Admittedly, during the high temperature deformation, the mechanical and microstructural comprehension of dynamic processes evolving on the basis of various processing situation is of much necessity to assess hot workability of metals<sup>[1]</sup>. At present, numerical simulation technology such as the finite element method (FEM) is extensively employed to investigate the metal deformation. As a result, the accuracy of the constitutive equations has come to be the critical point to enhance the reliability of the numerical simulation<sup>[2]</sup>. Meanwhile, a processing map using dynamic materials model (DMM) is also extensively adopted to identify the deformation processing parameters for hot working. Recently, processing maps have been established to improve the hot working processes of the metal alloys. The “safe” or “unsafe” regions during hot working procedures could be obtained by employing the processing map. Huang et al<sup>[3]</sup> investigated the high temperature deformation behavior of IN706 alloy using the processing map, and the validation of the processing map

was conducted by the EBSD microstructure analysis. Zhang et al<sup>[4]</sup> developed the hyperbolic-sine constitutive equation and processing map for Al-1.1Mn-0.3Mg-0.25RE alloy. Zhou et al<sup>[5]</sup> compared various instability criteria of the processing map, and obtained the optimal deformation parameters of superalloy GH4742. Rajamuthamilselvan and Ramanathan<sup>[6]</sup> identified the matrix crack, adiabatic shear band and debonding of 7075 Al/20% SiC<sub>p</sub> composite using the processing map. Based on the activation energy map and processing map, Sun et al<sup>[7]</sup> studied the high temperature processing parameters for powder metallurgy Ti-47Al-2Nb-2Cr alloy.

Owing to the superior combination of properties such as low density, excellent mechanical and corrosion-resistant properties, titanium alloy has been extensively employed in aerospace and aviation industries. Therefore, a considerable amount of research has been made to investigate the mechanical properties and deformation parameters of the titanium alloys. For example, Ning et al<sup>[8]</sup> investigated the

Received date: May 18, 2018

Foundation item: Industrial Science and Technique Key Project of Shaanxi Province (2016GY-207); Innovation Foundation of Western Materials (XBCL-3-19); Pre-research Foundation of Jinchuan Company-Xi'an University of Architecture and Technology (YY1501); Project of International Cooperation and Exchange of Shaanxi Provincial (2016 KW-054)

Corresponding author: Cai Jun, Ph. D., Associate Professor, Shaanxi Engineering Research Center of Metallurgical, School of Metallurgical Engineering, Xi'an University of Architecture and Technology, Xi'an 710055, P. R. China, E-mail: [caijun@xauat.edu.cn](mailto:caijun@xauat.edu.cn)

Copyright © 2018, Northwest Institute for Nonferrous Metal Research. Published by Elsevier BV. All rights reserved.

dynamic softening behavior of a dual-phase titanium alloy (TC18 alloy) during hot deformation. Sadeghpour et al.<sup>[9]</sup> designed a new kind of multi-element  $\beta$  titanium alloy with yield strength of 750 MPa, strain hardening rate of 1800 MPa and uniform elongation 19%. On the basis of hot uniaxial tensile tests and theoretical analysis, Ma et al.<sup>[10]</sup> investigated the hot formability of TA15 titanium alloy sheet. However, the characterization on the deformation ability of TA7 titanium alloy ( $\alpha$ -type alloy) has not been conducted in previous study.

This study mainly aims to investigate the elevated temperature deformation behavior of TA7 titanium alloy. Therefore, isothermal hot compression tests were carried out within the temperature range of 1123~1273 K and strain rate range of 0.001~1 s<sup>-1</sup>. Then the constitutive equation and processing map are developed to enhance the processing parameters of TA7 titanium alloy.

## 1 Experiment

The chemical composition (wt%) of as-received TA7 titanium alloy investigated in this research is: Al 5.6, Sn 2.5, Fe 0.27, Si 0.11, and Ti bal. To conduct the high temperature compression experiments, the cylindrical specimens which have a diameter of 10 mm and a height of 15 mm were used (as shown in Fig.1). Each specimen was heated to the deformation temperature at a rate of 10 K/s and then kept for 5 min. Thereafter, the tests of isothermal compression were conducted at the strain rates of 0.001, 0.01, 0.1 and 1 s<sup>-1</sup> and the temperatures of 1123, 1173, 1223 and 1273 K on a Gleeble-3800 simulator. The temperatures of the specimens decreased to room temperature in water after deformation. Besides, the strain-stress curves were documented mechanically in isothermal compression.

## 2 Results and Discussion

### 2.1 Flow stress

The flow stress curves at the deformation temperature of 1173 K and strain rate of 0.01 s<sup>-1</sup> can be found in Fig.2. According to the figures, the flow stress is severely affected by the deformation temperature and the strain rate. From the start of deformation, the flow stress rises rapidly with the increase of the deformation. Then, there exists a slow flow



Fig.1 Typical photos of the specimens before and after isothermal compression tests

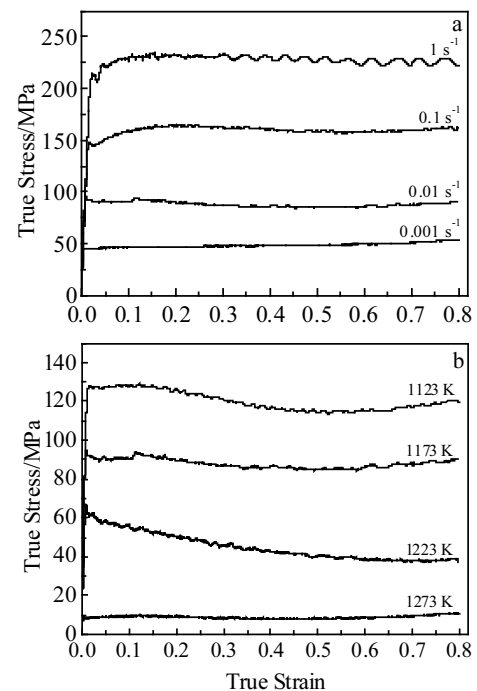


Fig.2 Flow stress curves of TA7 titanium alloy at the deformation conditions of 1173 K (a) and 0.01 s<sup>-1</sup> (b)

softening stage. Afterwards, a steady-state flow at the large strain follows, which is under most deformation conditions. In Fig.2b, it shows that the flow stress gradually decreases with the increase of the strain at the temperature of 1123, 1173 and 1223 K.

### 2.2 Constitutive equation

Under high temperature conditions, the flow stress  $\sigma$  of metal materials can be expressed as:

$$\sigma = f(\varepsilon, \dot{\varepsilon}, T, C, S) \quad (1)$$

where  $\varepsilon$  refers to true strain,  $\dot{\varepsilon}$  refers to strain rate (s<sup>-1</sup>),  $T$  indicates the absolute temperature (K),  $C$  is for the chemical composition of material, and  $S$  is for the microstructure of material. Obviously, during the deformation, no change is found in the composition. In the mean time, the microstructure of metal material could be reflected from the deformation state of the current deformation condition. Besides, it is consistently changed with the deformation parameters<sup>[11]</sup>. Therefore, the parameters  $C$  and  $S$  can be ignored, and Eq. (1) can be indicated as:

$$\sigma = f(\varepsilon, \dot{\varepsilon}, T) \quad (2)$$

There also exists another form to express the effect of the deformation parameters such as strain, strain rate and the deformation temperature on the flow stress<sup>[12]</sup>:

$$\sigma = \sigma_0 f_\varepsilon f_{\dot{\varepsilon}} f_T \quad (3)$$

where  $\sigma_0$  is the initial stress of TA7 titanium alloy under existing experimental situations;  $f_\varepsilon$ ,  $f_{\dot{\varepsilon}}$  and  $f_T$  are the influential coefficients of the strain, the strain rate and the deformation temperature, respectively. Then, with the natural

logarithms of both sides of Eq.(3), Eq.(4) can be derived as follows:

$$\ln \sigma = \ln \sigma_0 + \ln f_\epsilon + \ln f_{\dot{\epsilon}} + \ln f_T \quad (4)$$

It can be found from Eq.(3) to Eq.(4) that the coupled effects between the deformation parameters are ignored in the constitutive equation, which may reduce the accuracy of the developed constitutive equation. Therefore, the converged weights  $\omega$  are introduced for the purpose of describing the independent and combined effects of the deformation parameters. With the consideration of the converged weights  $\omega$ , the Eq. (5) can be derived<sup>[13]</sup>:

$$\ln \sigma = \ln \sigma_0 + \omega_\epsilon \ln f_\epsilon + \omega_{\dot{\epsilon}} \ln f_{\dot{\epsilon}} + \omega_T \ln f_T \quad (5)$$

And the constitutive equation for TA7 titanium alloy is given as follows:

$$\sigma = \sigma_0 \cdot f_\epsilon^{\omega_\epsilon} \cdot f_{\dot{\epsilon}}^{\omega_{\dot{\epsilon}}} \cdot f_T^{\omega_T} \quad (6)$$

In order to determine the material constants, the mean flow stress values  $\bar{\sigma}$  are employed.  $\bar{\sigma}_\epsilon$  refers to the mean value of flow stress at all temperatures and strain rates,  $\bar{\sigma}_{\dot{\epsilon}}$  is the mean value of the flow stress at all temperatures and strain, and  $\bar{\sigma}_T$  denotes the mean value of flow stress at all strain and strain rates.  $\bar{\sigma}_\epsilon$ ,  $\bar{\sigma}_{\dot{\epsilon}}$  as well as  $\bar{\sigma}_T$  can be expressed as follows:

$$\begin{cases} \bar{\sigma}_\epsilon = \sum_{T-\dot{\epsilon}} \sigma / (K_T \cdot K_{\dot{\epsilon}}) \\ \bar{\sigma}_{\dot{\epsilon}} = \sum_{T-\epsilon} \sigma / (K_T \cdot K_\epsilon) \\ \bar{\sigma}_T = \sum_{\epsilon-\dot{\epsilon}} \sigma / (K_\epsilon \cdot K_{\dot{\epsilon}}) \end{cases} \quad (7)$$

where  $K_\epsilon$ ,  $K_{\dot{\epsilon}}$ , and  $K_T$  are the levels of the strain, the strain rate, and the deformation temperature, respectively. The values of strain are chosen from 0.1 to 0.8 with an interval of 0.1, the strain rates are selected as 0.001, 0.01, 0.1, and 1 s<sup>-1</sup>, and the temperatures are selected as 1123, 1173, 1223 and 1273 K. Therefore, the values of  $K_\epsilon$ ,  $K_{\dot{\epsilon}}$ , and  $K_T$  are 8, 4 and 4, respectively. Fig.3 demonstrates the relationship between  $\bar{\sigma}_\epsilon$ -strain,  $\ln \bar{\sigma}_{\dot{\epsilon}} - \ln \dot{\epsilon}$  and  $\bar{\sigma}_T - T$ . A fourth fit can be used to depict the relationship between  $\bar{\sigma}_\epsilon$  and strain. In addition, linear fit can be applied to indicate the relationship of  $\ln \bar{\sigma}_{\dot{\epsilon}} - \ln \dot{\epsilon}$  and  $\bar{\sigma}_T - T$ , as given in Eqs. (8), (9) and (10).

$$\bar{\sigma}_\epsilon = 48.565 + 28.786\epsilon - 147.24\epsilon^2 + 228.32\epsilon^3 - 110.9\epsilon^4 \quad (8)$$

$$\ln \bar{\sigma}_{\dot{\epsilon}} = 5.23079 + 0.23875 \ln \dot{\epsilon} \quad (9)$$

$$\bar{\sigma}_T = 1331.46 - 1.02994T \quad (10)$$

Eq. (3) is rewritten as:

$$f_\epsilon f_{\dot{\epsilon}} f_T = \frac{\sigma}{\sigma_0} \quad (11)$$

Eqs.(8)~(10) are used to regress the equations of  $f_\epsilon$ ,  $f_{\dot{\epsilon}}$  and  $f_T$ . On the basis of Eq. (11), the values of  $f_\epsilon$ ,  $f_{\dot{\epsilon}}$  and  $f_T$  at different strain can be achieved from  $\bar{\sigma}_\epsilon/\bar{\sigma}_0$ ,  $\bar{\sigma}_{\dot{\epsilon}}/\bar{\sigma}_0$  and  $\bar{\sigma}_T/\bar{\sigma}_0$ . Besides,  $\bar{\sigma}_0$  is the value of mean flow stress at the minimum level of each factor (i.e. stain 0.1, strain rate 0.001 s<sup>-1</sup>, and temperature 1123 K in this study), which can be found in Eqs. (11) to (14).

$$f_\epsilon = 0.96771 + 0.57271\epsilon - 2.93114\epsilon^2 + 4.54573\epsilon^3 - 2.20795\epsilon^4 \quad (12)$$

$$f_{\dot{\epsilon}} = \exp(1.64923 + 0.23875 \ln \dot{\epsilon}) \quad (13)$$

$$f_T = 7.61538 - 5.8908(T/1000) \quad (14)$$

It is commonly accepted that the multivariate regression analysis (MRA) is considered as a highly flexible system for the examination of the relationship between a collection of independent variable and a dependent variable. Additionally, correction coefficient  $\sigma_0$  and the converged weights  $\omega$  can be obtained based on the least-squares regression on the basis of the independent variables  $\ln(f_\epsilon)$ ,  $\ln(f_{\dot{\epsilon}})$ ,  $\ln(f_T)$  as well as the dependent variable  $\ln \sigma$ . By conducting the multivariate regression test, the values of  $\sigma_0$  and  $\omega$  are acquired in Table 1.

According to Fig.4, by comparing the experimental and the predicted flow stress data, the developed constitutive equation of TA7 titanium alloy at high temperatures is confirmed. Obviously, the calculated data obtained from the constitutive equation can trace the experimental flow stress data of TA7 titanium alloy.

### 2.3 Processing map

The processing map on the basis of the DMM has proved to be a beneficial instrument in optimizing the hot working processing parameters of metal materials. Using processing map, the “safe” or “unsafe” regions in the hot deformation can be

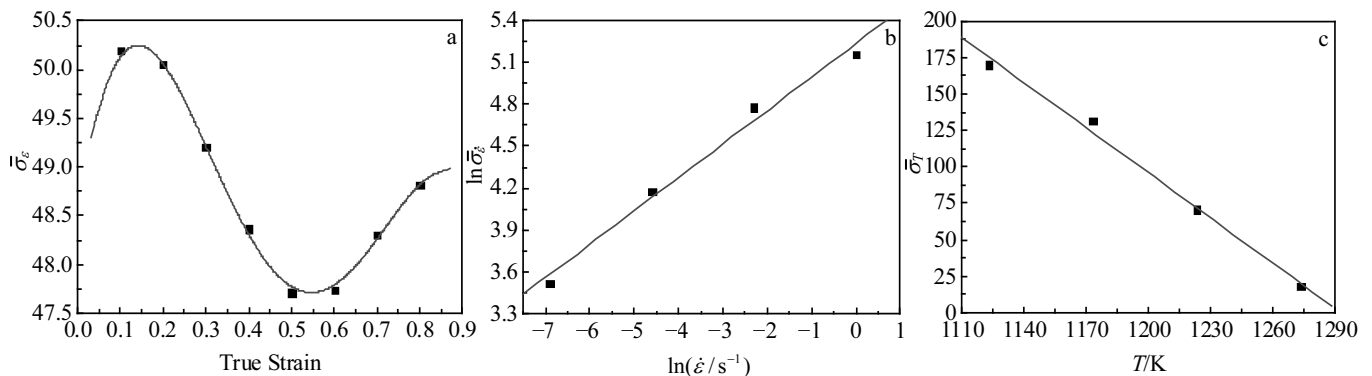


Fig.3 Relationship between  $\bar{\sigma}_\epsilon$ -strain (a),  $\ln \bar{\sigma}_{\dot{\epsilon}} - \ln \dot{\epsilon}$  (b) and  $\bar{\sigma}_T - T$  (c)

**Table 1** Values of  $\sigma_0$  and  $\omega$  obtained by MRA

$\sigma_0$	$\omega_\varepsilon$	$\omega_\dot{\varepsilon}$	$\omega_T$
63.94	1.340	1.106	1.13

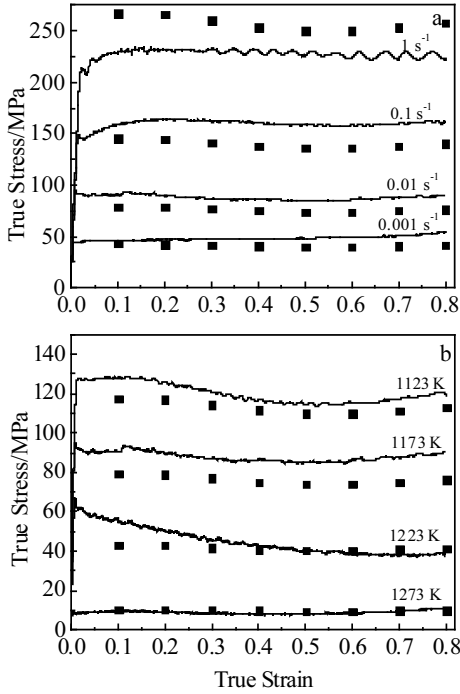


Fig.4 Comparison between the experimental and the predicted flow stress of TA7 titanium alloy under the deformation conditions of 1173 K (a) and 0.01 s<sup>-1</sup> (b)

easily obtained in accordance with instability criterion. Based on DMM, the power per unit volume  $P$  obtained from the work-piece during plastic flow processes is depicted as follows<sup>[14]</sup>:

$$P = \sigma \dot{\varepsilon} = \int_0^\sigma \dot{\varepsilon} d\sigma + \int_0^\varepsilon \sigma d\varepsilon = J + G \quad (15)$$

where  $G$  is dissipater content which represents the power scattered by plastic work, and  $J$  is dissipater co-content which is the work in association with the metallurgical mechanisms such as DRV, DRX, and internal fractures<sup>[15]</sup>.

The efficiency of power dissipation  $\eta$  can express power-dissipation capacity of the metal materials, which is shown as follows:

$$\eta = \frac{J}{J_{\max}} = \frac{2m}{m+1} \quad (16)$$

where  $\eta$  refers to a dimensionless parameter, which represents the efficiency of the energy dissipation based on microstructure evolution;  $m$  is the strain rate sensitivity. According to Fig.5,  $m$  could be obtained through differentiating the three-order polynomial fitting line of  $\ln\sigma$  and  $\ln\dot{\varepsilon}$  plots. The values of  $\eta$  are dependent on  $m$ , and it can reflect the microstructural evolution during the high temperature

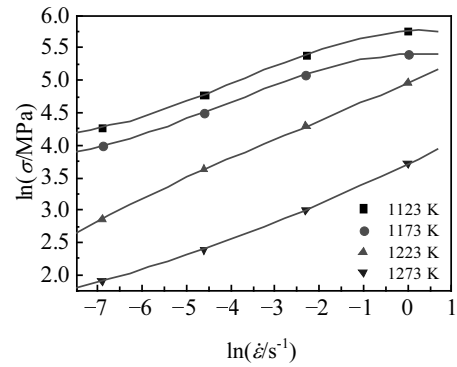


Fig.5 Relationship between  $\ln\sigma$  and  $\ln\dot{\varepsilon}$  at the strain of 0.8

deformation. Therefore, the microstructural changes of TA7 titanium alloy could be predicted through analyzing the values of  $\eta$  under the certain deformation condition, which is further verified by the microstructure observation<sup>[16]</sup>.

Thereafter, a continuum criterion for the occurrence of flow instabilities can be acquired regarding another dimensionless parameter  $\xi$ , which is expressed as:

$$\xi(\dot{\varepsilon}) = \frac{\partial \ln(\frac{m}{m+1})}{\partial \ln \dot{\varepsilon}} + m < 0 \quad (17)$$

The domains, in which the values of  $\xi$  are less than zero, can be regarded as the instability region. Then, based on Eqs. (16) and (17), the processing map of TA7 titanium alloy is obtained (as shown in Fig.6). The numbers on the contour lines indicate the values of the efficiency of power dissipation, and the dashed as well as non-dashed regions give the unstable flow and the reasonable deformation regions, respectively.

Generally, the high efficiency of power dissipation  $\eta$  means an optimal deformation condition. Nevertheless, due to some variations of instability, the high efficiency of the power dissipation does not essentially indicate better workability<sup>[17]</sup>. Only those regions in consistence with both the higher efficiency as well as stability regions can be considered as the optimal deformation parameters<sup>[7]</sup>. From Fig.6, the best processing parameters for the TA7 alloy are associated with a

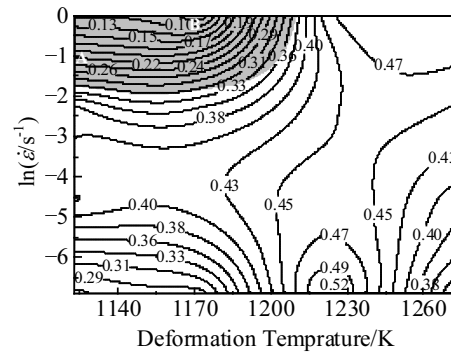


Fig.6 Processing map of TA7 titanium alloy

deformation temperature of 1223 K and a strain rate of  $0.001 \text{ s}^{-1}$ . Besides, the microstructure of TA7 titanium alloy under this deformation condition can be found in Fig.7. The figure shows the fine equiaxed primary  $\alpha$  phase of TA7 titanium alloy. During hot deformation, the stable fine  $\alpha$ - $\alpha$  phase interfaces can slide, reflecting the optimal deformation domain for TA7 titanium alloy.

Meanwhile, according to Fig.6, the instability domain locates at the lower temperature-higher strain rate region within the temperature range from 1123 K to 1219 K and the strain rate range from  $0.077 \text{ s}^{-1}$  to  $1 \text{ s}^{-1}$ . Similar results were reported in IMI 685 (a near- $\alpha$  titanium alloy)<sup>[18]</sup>, Ti-6.0Al-7.0Nb alloy<sup>[19]</sup>, Ti-15-3 titanium alloy<sup>[20]</sup>, and so on. Fig.8 shows

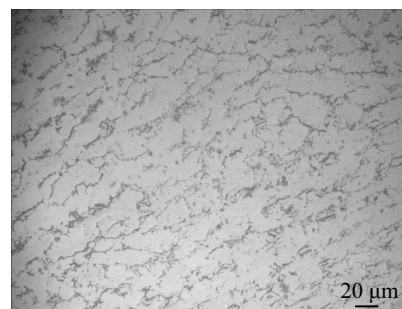


Fig.7 Microstructure of TA7 titanium alloy at the temperature of 1223 K and strain rate of  $0.001 \text{ s}^{-1}$

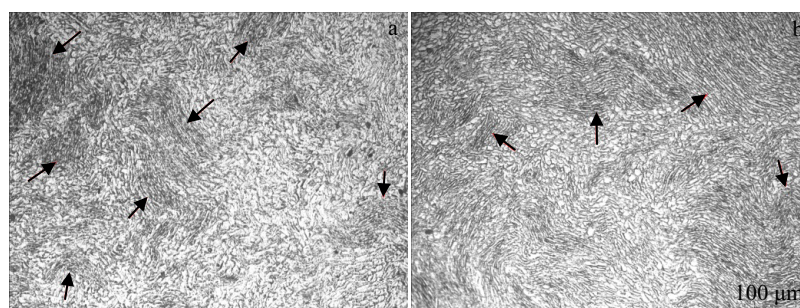


Fig.8 Microstructures of TA7 titanium alloy at temperature of 1123 K and strain rate of  $0.1 \text{ s}^{-1}$  (a) and temperature of 1173 K and strain rate of  $1 \text{ s}^{-1}$  (b)

the microstructure of the TA7 titanium alloy at 1123 K with the strain rate of  $0.1 \text{ s}^{-1}$  (position A in Fig.6) and the temperature of 1173 K with strain rate of  $1 \text{ s}^{-1}$  (position B in Fig.6), corresponding to the instability domain of the processing map.

The figures show that after lower temperature compression, the specimens exhibit obvious inhomogeneous deformation. The microstructure of the specimens shows that high strain rate and low temperature will lead to the occurrence of flow localizations (arrows in Fig.8a and 8b). This phenomenon may be caused by the fact that the insufficient plastic deformation time can lead to a decrease in the flow stress locally with further straining, thus consequently making slip localized<sup>[20]</sup>. Meanwhile, lower values of  $\eta$  can also reduce the tendency for flow localization<sup>[21]</sup>. It can be seen from the processing map that the values of  $\eta$  corresponding to the instability domain are located at the lower region, which indicates that a large proportion of the plastic power is changed into heat and is dissipated by means of temperature rise<sup>[19]</sup>. Therefore, the material has a poor workability in this region.

### 3 Conclusions

1) With the change of deformation temperature and the strain rate, the flow stress of TA7 titanium alloy is sensitive.

2) A modified parallel constitutive model is presented to depict the flow stress as a role of the strain rate, deformation

temperature and true strain. Through comparison, the predictability of the developed constitutive equation is proved.

3) According to the processing map, the deformation temperature of 1223 K and strain rate of  $0.001 \text{ s}^{-1}$  are the optimal processing parameters for the TA7 alloy. Besides, the instability region is the deformation temperatures ranging from 1123 K to 1219 K as well as the strain rate ranging from  $0.077 \text{ s}^{-1}$  to  $1 \text{ s}^{-1}$ .

### References

- 1 Momeni A, Dehghani K. *Materials Science and Engineering A*[J], 2010, 527(21-22): 5467
- 2 Cai J, Wang K S, Miao C P et al. *Materials and Design*[J], 2015, 65: 272
- 3 Huang S, Wang L, Lian X T et al. *Acta Metallurgica Sinica*[J], 2014, 27(2): 198
- 4 Zhang Tian, Tao Yourui, Wang Xueyin. *Transactions of Nonferrous Metals Society of China*[J], 2014, 24(5): 1337
- 5 Zhou G, Ding H, Cao F R et al. *Journal of Materials Science and Technology*[J], 2014, 30(3): 217
- 6 Rajamuthamilselvan M, Ramanathan S. *Journal of Materials Engineering and Performance*[J], 2012, 21(2): 191
- 7 Sun Y, Wan Z P, Hu L X et al. *Materials and Design*[J], 2015, 86: 922
- 8 Ning Y Q, Xie B C, Liang H Q et al. *Materials and Design*[J],

- 2015, 71: 68
- 9 Sadeghpour S, Abbasi S M, Morakabati M et al. *Scripta Materialia*[J], 2018, 145: 104
- 10 Ma B L, Wu X D, Li X J et al. *Materials and Design*[J], 2016, 94: 9
- 11 Zhang C, Zhang L W, Shen W F et al. *Journal of Materials Engineering and Performance*[J], 2015, 24(1): 149
- 12 Yuan Z W, Li F G, Qiao H J et al. *Materials Science and Engineering A*[J], 2013, 578: 260
- 13 Xiao M L, Li F G, Zhao W et al. *Materials and Design*[J], 2012, 35: 184
- 14 Cai J, Shi J M, Wang K S et al. *International Journal of Materials Research*[J], 2017, 108(7): 527
- 15 Luo J, Li M Q, Li H et al. *Materials Science and Engineering A*[J], 2009, 505: 88
- 16 Medeiros S C, Prasad Y V R K, Frazier W G et al. *Materials Science and Engineering A*[J], 2000, 293(1-2): 198
- 17 Kong Y K, Chang P P, Li Q et al. *Journal of Alloys and Compounds*[J], 2015, 622: 738
- 18 Cai J, Wang K S, Wang W. *Rare Metal Materials and Engineering*[J], 2016, 45(10): 2549
- 19 Prasad Y V R K, Seshacharyulu T. *Materials Science and Engineering A*[J], 1998, 243: 82
- 20 Liu Y H, Ning Y Q, Yao Z K et al. *Journal of Alloys and Compounds*[J], 2014, 587: 183
- 21 Zhang J Q, Di H S, Wang H T et al. *Journal of Materials Science*[J], 2012, 47(9): 4000

## TA7 钛合金高温变形行为研究

杨晓康, 王快社, 史佳敏, 王 萌, 蔡 军, 王庆娟, 刘莹莹  
(西安建筑科技大学 陕西省冶金工程技术研究中心, 陕西 西安 710055)

**摘 要:** 为了分析 TA7 钛合金的热变形工艺参数, 通过高温压缩试验对 TA7 钛合金的高温变形行为进行了研究。试验温度为 1123~1273 K, 应变速率为  $0.001\sim 1\text{ s}^{-1}$ 。此外, 提出了一种修正并联本构模型用来分析应变速率、变形温度及应变对流动应力的影响。然后, 基于动态模型, 建立了 TA7 钛合金的热加工图, 并通过微观组织分析对加工图的准确性进行了验证。结果表明, TA7 钛合金合理的工艺参数为变形温度 1223 K, 应变速率  $0.001\text{ s}^{-1}$ , 而其非稳态区域位于低温高应变速率区。

**关键词:** TA7 钛合金; 高温变形行为; 本构方程; 加工图

---

作者简介: 杨晓康, 男, 1982 年生, 博士生, 西安建筑科技大学冶金工程学院, 陕西省冶金工程技术研究中心, 陕西 西安 710055, E-mail: yangxiaokang2000@163.com